

1 **Environmental and inoculum effects on epidemiology of bacterial spot disease of stone fruits and**
2 **development of a disease forecasting system**

3

4 G. Morales, C. Moragrega, E. Montesinos and I. Llorente

5 Institute of Food and Agricultural Technology-XaRTA-CIDSAV, University of Girona. C/ Maria Aurèlia

6 Capmany 61, 17003 Girona. Spain.

7

8 * Corresponding author: C. Moragrega

9 E-mail: concepcio.moragrega@udg.edu

10 **Key words:** epiphytic growth, incubation period, inoculum potential, growth rate, leaf wetness, temperature.

11

12 **Abstract**

13

14 Bacterial spot disease of stone fruits, caused by *Xanthomonas arboricola* pv. *pruni*, is of high economic
15 importance in the major stone-fruit-producing areas worldwide. A better understanding of disease epidemiology
16 can be valuable in developing disease management strategies. The effects of weather variables (temperature and
17 wet/dry period) on epiphytic growth of *X. arboricola* pv. *pruni* on *Prunus* leaves were analyzed, and the
18 relationship between inoculum density and temperature on disease development was determined and modeled.
19 The information generated in this study, performed under controlled environmental conditions, will be useful to
20 develop a forecasting system for *X. arboricola* pv. *pruni*.

21 Optimal temperature for growth of epiphytic populations ranged from 20 to 30°C under leaf wetness. In
22 contrast, multiplication of epiphytic populations was not only interrupted under low relative humidity (RH) (<
23 40%) at 25°C, but also resulted in cell inactivation, with only 0.001% initial cells recovered after 72 h
24 incubation. A significant effect of inoculum density on disease severity was observed and 10^6 CFU/ml was
25 determined as the minimal infective dose for *X. arboricola* pv. *pruni* on *Prunus*. Infections occurred at
26 temperatures from 15 to 35°C, but incubation at 25 and 30°C gave the shortest incubation periods (7.7 and 5.9
27 days respectively). A model for predicting disease symptom development was generated and successfully
28 evaluated, based on the relationship between disease severity and the accumulated heat expressed in cumulative
29 degree day (CDD). Incubation periods of 150, 175 and 280 CDD were required for 5, 10 and 50% of disease
30 severity, respectively.

31 **Introduction**

32 *Xanthomonas arboricola* pv. *pruni* (Vauterin et al. 1995) (synonym, *Xanthomonas campestris* pv. *pruni* [Smith]
33 Dye) is a Gram-negative plant-pathogenic bacterium that causes bacterial spot disease in stone fruits
34 (EPPO/CABI 1997; Palacio-Bielsa et al. 2010). The pathogen can affect all cultivated *Prunus* species and their
35 hybrids, but the most severe epidemics have been reported in Japanese plum (*Prunus salicina*), *P. japonica* and
36 hybrids, and in peach and nectarines, *P. persica* and hybrids (Ritchie 1995). The disease, first described for
37 Japanese plum in the USA in 1903 (Smith 1903), is today distributed throughout the major stone-fruit-producing
38 areas of the world (EPPO 2017).

39 *X. arboricola* pv. *pruni* is a harmful organism relevant to the European Union (EU), according to the Council
40 Directive 2000/29/EC, and a quarantine pathogen, in the A2 list, for the European Plant Protection Organisation
41 (EPPO) (EPPO/CABI 1997). The pathogen is spreading in many European countries, which have reported local
42 outbreaks (EPPO 2017; Scortichini 2010).

43 Disease symptoms include necrotic angular spots on leaves, spots or sunken lesions on fruit and stem canker.
44 Heavy infections lead to severe defoliation, mainly on peach and nectarine (Stefani 2010), resulting in weakened
45 trees. The disease produces a negative economic impact because of the decrease in quality and marketability of
46 affected fruits, a reduction of tree productivity and an increase in production costs (Janse 2012).

47 As no effective chemical control is available for this disease, quarantine measures are needed to avoid the
48 introduction and dissemination of *X. arboricola* pv. *pruni*. These include phytosanitary certification of plant
49 propagation material, nursery and orchard inspections and elimination of contaminated plant material. In
50 affected areas, control of this pathogen is currently limited to preventative copper spray applications at late
51 dormant stage and early in the growing season (Ritchie 2004; Stefani 2010; Wert et al. 2006). The use of
52 antibiotics, mainly oxytetracycline and streptomycin, is restricted to countries where they are registered for
53 agronomic uses (Stockwell and Duffy 2012; Vanneste et al. 2005). Appropriate and rational timing of copper
54 sprays is critical to increase the efficacy of disease control and to overcome the limitations that have been
55 related to the use of this compound: moderate efficacy, plant phytotoxicity (Lalancette and McFarland 2007)
56 and risk of development of copper resistance in the bacterium (Giovanardi et al. 2016; Vanneste et al. 2005).
57 Therefore, an effective control strategy for this disease should take into account the use of a reliable disease
58 forecasting model. The forecaster would be used as a decision support system to guide disease surveillance tasks
59 for early detection of outbreaks or spread of the disease, and copper applications for disease management.

60 Some forecasting systems for plant diseases caused by bacteria, such as Maryblyt (Lightner and Steiner 1992),
61 CougarBlight (Smith 1993), and Billing's integrated system (BIS95) (Billing 1999) for fire blight in apple and
62 pear, caused by *Erwinia amylovora*, and the risk model for bacterial canker of kiwifruit, caused by
63 *Pseudomonas syringae* pv. *actinidiae* (Beresford et al. 2017) are based in two separate processes. The first
64 involves bacterial multiplication to provide inoculum, which is temperature-dependent and requires the presence
65 of free water (surface wetness or high RH). The second process is related to infection occurrences and disease
66 development, and depends on weather parameters, mainly temperature, leaf wetness, and RH. A similar
67 approach is proposed to develop a forecasting system for bacterial spot disease of stone fruits.

68 Previously, we determined and modeled the effect of temperature on growth of *X. arboricola* pv. *pruni* *in vitro*
69 (Morales et al. 2017). The model can be used to predict the inoculum potential of this pathogen. However, *in*
70 *vitro* assays do not reflect the natural conditions for epiphytic bacterial growth on plant organs, and the model
71 should be validated or refined on host plants. Some bacterial growth models included in disease forecasting
72 systems consider bacterial multiplication only when moisture is present (Kim et al. 2014; Beresford et al. 2017).

73 Although temperature is the most important weather parameter for bacterial growth, knowledge of the effect of
74 dry periods (with low RH) on the dynamics of epiphytic populations could provide additional information for
75 modelling the epiphytic growth of *X. arboricola* pv. *pruni*.

76 *X. arboricola* pv. *pruni* may survive as an epiphyte on *Prunus* hosts in orchards or nurseries, associated with
77 buds and leaf scars, which act as overwintering sites and sources of primary inoculum for spring infections
78 (Anonymous, 2006). The population density is critical to forecast disease development, and the minimum
79 pathogen population size to cause infections, also known as the infection threshold, is a key parameter for
80 estimating the inoculum potential. The infection threshold has been determined for bacterial plant pathogens: at
81 least 10^5 - 10^6 bacterial cells/flower are needed for *Erwinia amylovora* infection on apple (Billing 1984),
82 *Pseudomonas syringae* pv. *syringae* needed more than 10^4 bacterial cells/g leaf fresh weight for bean infection
83 (Lindemann 1984), and the threshold for *X. campestris* pv. *vesicatoria* infection on hot pepper has been
84 determined as 5×10^5 bacterial cells/leaf (Kim et al. 2014). Regarding *X. arboricola* pv. *pruni*, 16 - 18 bacterial
85 cells were apparently required to induce a single lesion on peach leaves, and inoculum densities from 10^6 to 10^8
86 CFU/ml were necessary to cause generalized chlorosis and necrosis on peach leaves under controlled conditions
87 (Civerolo 1975). However, the infective dose for this pathogen needs to be confirmed, as the efficiency of
88 different inoculation techniques is variable (Socquet-Juglard et al. 2012). The infection threshold for *X.*

89 *arboricola* pv. *pruni* could be integrated into the bacterial growth model to predict when the inoculum potential
90 is sufficient to initiate infections.

91 Weather parameters play an important role in the infection of *Prunus* by *X. arboricola* pv. *pruni* and in the
92 disease development. Moderate temperatures and leaf wetness are required for this bacterium to penetrate the
93 host cells through natural openings or wounds (EPPO/CABI 1997; Garcin et al. 2011a; Goodman 1976; Morales
94 et al. 2016; Zehr et al. 1996). Thus, the combined effects of wetness period duration and temperature on
95 infection of *Prunus* by *X. arboricola* pv. *pruni* were analyzed under controlled environment conditions and an
96 infection risk model was developed (Morales et al. 2018). The model was successfully validated under
97 greenhouse conditions and, after field evaluation, it could be used to forecast the *X. arboricola* pv. *pruni*
98 infection events on *Prunus*. Plant disease forecasting models can not only predict the onset of a disease, but also
99 predict disease symptom development. Since temperature affects the development rate of many organisms, the
100 measure of accumulated heat (physiological time) has been used to predict the incubation period for disease
101 symptom expression in forecasting systems such as Maryblyt (Lightner and Steiner 1992) and BIS95 (Billing
102 1999). As the incubation period for bacterial spot disease of stone fruits is mainly affected by temperature and
103 inoculum dose (Battilani et al. 1999; Randhawa and Civerolo 1985; Zehr et al. 1996), it is important to know the
104 relationship between these factors and disease progress and symptom development prior to inclusion into the
105 forecasting system of this disease.

106 This study was aimed at increasing knowledge of the effects of weather parameters and inoculum density on the
107 dynamics of epiphytic populations of *X. arboricola* pv. *pruni* and on infection and disease symptom
108 development on *Prunus* leaves, under controlled environmental conditions. The objectives were to: (i) determine
109 the effect of temperature and relative humidity on *X. arboricola* pv. *pruni* growth on *Prunus* leaf surface; (ii)
110 evaluate the effect of inoculum density of *X. arboricola* pv. *pruni* on infection on *Prunus* leaves; and (iii)
111 analyze the effect of temperature and inoculum density on disease progress and symptom development.

112

113 **Materials and methods**

114 **Plant material**

115 Potted plants of the peach-almond hybrid (*Prunus persica* x *P. amygdalus*) GF-677, commonly used as
116 rootstock, obtained by micropropagation (Agromillora Catalana, Subirats, Spain) and nectarine plants cv. Big
117 Top (Certiplant, S.L., Lleida, Spain), both susceptible to bacterial spot disease of stone fruits, were used.
118 Micropropagated GF-677 plants were used in whole plant assays, and in some detached leaf assays, whereas

119 nectarine plants were only used in detached leaf assays, depending on the supplier availability. Plants were
120 grown in 0.5-l pots filled with a commercial peatmoss/vermiculite/perlite potting mix (type BVU, Prodeasa,
121 Girona, Spain) in the greenhouse and fertilized once a week with a solution of 200 ppm N-P-K (20-10-20).

122

123 **Pathogen**

124 *X. arboricola* pv. *pruni* strain CFBP 5563 isolated from peach in France (CIRM-CFBP: International Center for
125 Microbial Resources - French Collection for Plant-associated Bacteria, Beaucoz , France) was used in this
126 study. Bacteria were stored in stock tubes containing yeast-peptone-glucose broth (YPG) (Boudon et al. 2005)
127 supplemented with glycerol (20% wt/vol) at -70 C.

128 The strain *X. arboricola* pv. *pruni* CFBP 5563 was marked for rifampicin resistance (Rif^r) by growing on yeast-
129 peptone-glucose agar (YPGA) (Boudon et al. 2005) supplemented with 50 µg/ml rifampicin (YPGA+R) for 48
130 h at 27 C. Spontaneous mutant derivatives were selected and the stability of rifampicin resistance was confirmed
131 by subculturing five times on YPGA in the absence of antibiotic selection and, finally, on YPGA+R. Mutants
132 were routinely grown on YPGA+R (50 µg/ml rifampicin). The mutant strain CFBP 5563 Rif^r did not differ in
133 growth from the wild-type strain, neither *in vitro* nor *ex vivo* (data not shown). The strain CFBP 5563 Rif^r was
134 used in epiphytic growth assays.

135

136 **Effect of temperature on epiphytic growth of *X. arboricola* pv. *pruni* on *Prunus* leaves under wetness**

137 The epiphytic growth of *X. arboricola* pv. *pruni* at different temperatures under wetness was monitored on
138 leaves of the peach-almond hybrid GF-677 in a detached leaf assay, under controlled environmental conditions.
139 Bacterial suspensions of *X. arboricola* pv. *pruni* CFBP 5563 Rif^r mutant were prepared from 24 h cultures
140 grown at 27 C on YPGA+R by scraping bacterial colonies from the culture and adjusting them with sterile
141 distilled water to an optical density of 0.2 at $\lambda = 600$ nm (approximately 10⁸ CFU/ml). The bacterial suspensions
142 were serially diluted with sterile distilled water to obtain a final population density of 10⁴ CFU/ml. Viable
143 counts of the inoculum suspensions were determined by spreading 0.1 ml of appropriate 10-fold serial dilutions
144 on YPGA+R plates and incubating for 72 h at 27 C.

145 Leaves of the peach-almond hybrid GF-677 were collected from potted plants with actively growing shoots,
146 surface disinfected by immersion in 5% sodium hypochlorite solution for 30 s and rinsed three times with sterile
147 distilled water. The leaves were then inoculated by immersion in the bacterial suspension, placed on a grid in
148 plastic boxes filled with wet filter paper and sealed in moistened transparent polyethylene bags to maintain leaf

149 wetness. Inoculated leaves were incubated for 14 days at constant temperatures of 5, 10, 15, 20, 25, 30 or 35°C
 150 and a 12-h light photoperiod in controlled environment chambers (model MLR-350; Sanyo, Gunma, Japan),
 151 with a maximum variation of $\pm 1^\circ\text{C}$ for all temperatures. The temperature and RH inside the chamber was
 152 monitored and recorded using a HOBO® U23 Pro v2 temp/RH data logger (Onset Computer Corp, Pocasset,
 153 MA, USA). Leaves inoculated with sterile distilled water were used as negative control. Population densities of
 154 *X. arboricola* pv. *pruni* CFBP 5563 Rif^r on GF-677 leaf surface were assessed at 0, 12, 24 h and 2, 3, 4, 7, 9, 11
 155 and 14 days after inoculation. Three replicates of five leaves were used for each sampling time and temperature.
 156 A completely randomized experimental design was used and the experiment was performed twice. For bacterial
 157 population density determination, each sample of five leaves was placed in a sterile plastic bag containing 50 ml
 158 of extraction buffer (7.10 g Na₂HPO₄, 2.72 g KH₂PO₄, and 1 g peptone per 1000 ml of distilled water) and
 159 ground in a lab blender (Stomacher, IUL Instruments, Germany) for 5 minutes. Aliquots and serial dilutions
 160 were subsequently plated in duplicate on YPGA+R supplemented with 10 µg/ml econazole nitrate (to prevent
 161 fungal growth) and incubated for 72 h at 27°C. Results were expressed as CFU per gram of leaf fresh weight.
 162 Viable count data were plotted versus time, and three growth curves were obtained at each temperature per
 163 experiment. The modified Gompertz model (Zwietering et al. 1990) described by equation 1 was used to
 164 estimate the maximum specific growth rate and lag time for *X. arboricola* pv. *pruni* at each temperature:

$$\log_{10} N_t = \log_{10} N_0 + A \cdot \exp \left\{ -\exp \left[\frac{\mu_{\max} \cdot e}{A} \cdot (\text{lag} - t) + 1 \right] \right\} \quad \text{Equation 1}$$

166 where A is the logarithmic increase of bacterial population [\log_{10} (CFU/g)], e is $\exp(1)$, lag is the lag time (h),
 167 N_0 is the initial population density (CFU/g), N_t is the population density (CFU/g) at time t (h), and μ_{\max} is the
 168 maximum specific growth rate (h^{-1}). The modified Gompertz model was fitted to growth curves by nonlinear
 169 regression using R (R Development Core Team 2015) package nlstools (Baty et al. 2013). The goodness of fit of
 170 the model was assessed using the residual sum of squares (RSS). The effects of temperature on the growth rate
 171 was determined using the general linear model (GLM) procedure of SPSS v. 23.0 software (IBM Corp.,
 172 Armonk, NY), after confirmation of the homogeneity of variance and normality.

173
 174 **Effect of low RH on epiphytic population dynamics of *X. arboricola* pv. *pruni* on *Prunus* leaves**

175 The epiphytic population dynamics of *X. arboricola* pv. *pruni* on *Prunus* leaves under periods of low RH (<
 176 40%) was analyzed under controlled environment conditions. As it was assumed that cell inactivation depends
 177 on the duration of the dry period, regardless of temperature (Kim et al. 2014), the experiment was performed at
 178 25°C, optimal temperature for *X. arboricola* pv. *pruni* growth (Morales et al. 2017).

179 Bacterial suspensions of strain CFBP 5563 Rif^r were obtained from 24 h cultures grown at 27°C on YPGA+R as
180 described above, and adjusted to an optical density of 0.5 at 600 nm (about 10⁹ CFU/ml). Young leaves of
181 peach-almond hybrid GF-677 potted plants were collected, disinfected in a 5% sodium hypochlorite solution,
182 rinsed three times in sterile distilled water and inoculated by immersion in the bacterial suspension, as described
183 previously. Inoculated leaves were left to surface dry inside a laminar flow cabinet and placed on sterile filter
184 paper inside plastic boxes sealed in transparent polyethylene bags. Saturated calcium chloride (CaCl₂ 6 H₂O)
185 was used as drying agent to maintain a low RH (< 40%) inside the plastic boxes (Dhingra and Sinclair 1985).
186 Boxes with inoculated leaves were incubated for 72 h at 25°C and 12-h light photoperiod in a controlled
187 environment chamber (model MLR-350; Sanyo, Gunma, Japan), with a maximum variation of ±1°C. The
188 temperature and RH inside the chamber were monitored and recorded as described above. Leaves inoculated
189 with sterile distilled water were used as negative control. Three replicates of five leaves were sampled after 0, 6,
190 12, 24, 48 and 72 h of incubation and total viable counts were determined as described previously. The
191 experiment was performed three times. A completely randomized experimental design was used. Differences
192 between experiments on total viable counts were determined using the GLM procedure after confirmation of the
193 homogeneity of variance and normality.

194 Averaged viable count data of three replicates in an experiment were plotted against time to give survival curves
195 for *X. arboricola* pv. *pruni* CFBP 5563 Rif^r on *Prunus* leaves under dry periods. Different inactivation models
196 have been successfully applied in predictive microbiology to fit different shapes of bacterial survival curves
197 (Xiong et al. 1999), which can be used when pathogen populations decrease under dry conditions. Here, the
198 Cerf's model (Cerf 1977) (equation 2), which is suitable for fitting lineal survival curves and curves with a tail
199 (Xiong et al. 1999), was fitted to survival curves of *X. arboricola* pv. *pruni* CFBP 5563 Rif^r using the nonlinear
200 regression procedure of SPSS v. 23.0 software (IBM Corp., Armonk, NY). The Cerf model is expressed as:

$$201 \quad N_t = N_0 \times [f \times \exp(-k_1 t)] + (1 - f) \times \exp(-k_2 t) \quad \text{Equation 2}$$

202 where f and $(1 - f)$ are the initial proportion in the less resistant fraction and the more resistant fraction of the
203 population, respectively; k_1 and k_2 ($k_1 > k_2 \geq 0$) are the death rate constants for the less and the more resistant
204 fraction of the population, respectively; N_0 is the initial population density (CFU/ml); and N_t is the population
205 density (CFU/ml) at time t (h). The model goodness of fit was assessed using the root mean square error
206 (RMSE) and correlation coefficient (R^2) between experimental and predicted values.

207

208 **Effect of inoculum density of *X. arboricola* pv. *pruni* on disease severity on *Prunus* leaves**

209 A stock suspension on sterile distilled water of *X. arboricola* pv. *pruni* strain CFBP 5563 was obtained as
210 described previously from LB agar cultures grown for 72 h at 27°C and adjusted to an optical density of 0.5 at
211 600 nm (10^9 CFU/ml). The stock bacterial suspension was serially diluted 10-fold with sterile distilled water to
212 obtain suspensions ranging from 1×10^1 to 1×10^9 CFU/ml. Viable counts of the stock bacterial suspension were
213 determined by spreading 0.1 ml of appropriate dilutions on YPGA plates and incubating for 72 h at 27°C.
214 Leaves of nectarine cv. Big Top were collected from actively growing shoots in potted plants and disinfected as
215 described above. Three different inoculation methods were used: (i) leaf immersion in the bacterial suspension;
216 (ii) local infiltration of 25- μ l of bacterial suspension using a syringe without needle at four sites into the abaxial
217 surface in a leaf, two at each side of the mid-vein; and (iii) deposition of four 25- μ l drops of bacterial
218 suspension onto the reverse of a leaf. The same methods were repeated with sterile distilled water on different
219 leaves to serve as negative controls. Three replicates of three leaves were inoculated with each method per
220 inoculum concentration. Inoculated leaves were placed inside plastic boxes on moistened filter paper, covered
221 with a polyethylene bag to maintain high RH (> 98%) and incubated for 21 days at 25°C and 12-h light
222 photoperiod in a controlled environment chamber (model MLR-350; Sanyo, Gunma, Japan) with a maximum
223 variation of $\pm 1^\circ\text{C}$. A completely randomized experimental design was used. The experiment was performed
224 twice.
225 Disease severity was assessed 21 days after inoculation. Different disease severity indices (*I*) were established
226 depending on the inoculation method. For immersion, *I* ranged from 0 to 3, corresponding to a leaf area affected
227 by 0, 6, 12 or $\geq 24\%$, respectively (Battilani et al. 1999; Garcin et al. 2011b). For local infiltration and drop
228 deposition *I* ranged from 0 to 3 with 0, no infection; 1, necrosis restricted to the inoculation point; 2, necrosis
229 affecting the whole inoculated area; and 3, necrosis expanding through the leaf (Moragrega et al. 1998; Ruz et
230 al. 2008). Finally, disease severity (*S*) was calculated according to the equation: $S = (\sum_{i=1}^n I_n /$
231 $(N \times 3)) \times 100$, where I_n is the disease severity index in an inoculation site, *N* is the total number of inoculation
232 sites in a leaf, and 3 is the maximum severity index. The effects of inoculum density and inoculation method
233 were determined using the GLM procedure, after confirmation of the homogeneity of variance and normality,
234 and Tukey's HSD test was used for mean comparison.

235

236 **Effect of temperature and inoculum density on disease progress and symptom development**

237 A total of six temperatures (10, 15, 20, 25, 30 or 35°C) and three inoculum concentrations (1×10^4 , 1×10^6 and 1
238 $\times 10^8$ CFU/ml) were combined in a detached leaf assay performed under controlled environment conditions.

239 Bacterial suspensions in sterile distilled water of *X. arboricola* pv. *pruni* strain CFBP 5563 grown on LB plates
240 for 72 h at 27°C were obtained as described above and adjusted to an optical density of 0.2 at 600 nm (10^8
241 CFU/ml). Bacterial suspensions were serially 10-fold diluted in sterile distilled water to obtain inoculum
242 concentrations of about 10^4 , 10^6 CFU/ml, as well as the initial concentration of 10^8 CFU/ml. Cell density of
243 inoculum suspensions was confirmed by dilution plating on YPGA and incubation for 72 h at 27°C.

244 Young leaves of the peach-almond hybrid GF-677 were collected from potted plants with actively growing
245 shoots, and disinfected with sodium hypochlorite (5%) for 10 min, followed by rinsing three times with sterile
246 distilled water. Leaves were inoculated with bacterial suspensions of the corresponding inoculum concentration
247 by local infiltration of 25- μ l bacterial suspension, as described above. Four inoculations were performed in any
248 single leaf. Leaves inoculated with sterile distilled water were used as negative controls. Inoculated leaves were
249 placed on a grid in plastic boxes filled with wet filter paper, sealed in moistened transparent polyethylene bags
250 to maintain a high RH (> 98%), and incubated for 21 days at the corresponding constant temperature and 12-h
251 light photoperiod in a controlled environment chamber (model MLR-350; Sanyo, Gunma, Japan), with a
252 maximum variation of $\pm 1^\circ\text{C}$ for all temperatures. The temperature inside the growth cabinet was monitored and
253 recorded as described above. Disease severity was assessed daily on a 0 - 3 scale severity index (*I*) as previously
254 described, and disease severity (*S*) was calculated per leaf according to the formula indicated above. A
255 completely randomized experimental design was used. The treatment layout was a factorial arrangement with
256 six temperatures (10, 15, 20, 25, 30 and 35°C) and three inoculum densities (10^4 , 10^6 and 10^8 CFU/ml). Five leaf
257 replicates were used per temperature-inoculum density combination with four inoculation sites in a leaf. The
258 entire experiment was conducted twice.

259 Disease progress curves were obtained per temperature, inoculum concentration and replicate by plotting the
260 disease severity over time. The area under the disease progress curve (AUDPC) was calculated using the
261 midpoint (trapezoidal) rule method and standardized (SAUDPC) by dividing its value by the total length of
262 incubation (21 days) (Campbell and Madden 1990). The effects of experiment, temperature and inoculum
263 density on the incubation period (the time between inoculation and symptom development), final disease
264 severity (21 days after inoculation) and SAUDPC were determined using the GLM procedure and Tukey's HSD
265 test was used for mean comparison. Previously, the homogeneity of variance and normality were tested.

266 Cumulative degree days (CDD) with a threshold temperature of 0°C, were calculated daily as the sum of the
267 daily mean temperature from day 1 of incubation to the current day. Disease progress curves against CDD were
268 obtained for each temperature-inoculum density combination. The CDD-disease progress curves at optimal

269 temperatures (20, 25 and 30°C) and highest inoculum density (10^8 CFU/ml) were used for modeling the
270 symptom development of bacterial spot disease. Disease severity was standardized by dividing by 100 (y) and
271 transformed according to the monomolecular, $z = \ln[1/(1-y)]$; exponential, $z = \ln(y)$; logistic, $z = \ln[y/(1-y)]$; and
272 Gompertz, $z = -\ln[-\ln(y)]$ models (Table 3) (Campbell and Madden 1990) to obtain linear relationships between
273 disease severity (z) and CDD (independent variable). Only data points with disease severity $0 < S < 1$ were
274 included, since 0 and 1 are not defined in several of the model transformations. The four models (Table 3) were
275 fitted to data by linear regression. The goodness of fit of models were assessed by R^2 , mean square error (MSE),
276 and R^{2*} obtained from the relationship between predicted back-transformed values and observed values
277 (Campbell and Madden 1990). The upper and lower boundaries of the 95% confidence interval were also
278 calculated. The best fit model was selected for predicting the disease severity as a function of CDD and
279 proposed as a prediction model of symptom development.

280 The capacity of the model for predicting symptom development was analyzed in two additional independent
281 experiments on *Prunus* plants. Actively growing potted plants of the peach-almond hybrid GF-677 were
282 inoculated by spraying 5×10^8 CFU/ml suspensions of *X. arboricola* pv. *pruni* strain CFBP 5563, obtained as
283 described above, supplemented with 1 mg/ml diatomaceous earth (abrasive agent to favor bacterial infection).
284 Plants inoculated with sterile distilled water with the addition of diatomaceous earth were used as negative
285 controls. Inoculated plants were introduced into transparent plastic bags to maintain leaf wetness and incubated
286 for 24 h at 25°C under darkness in a controlled environment chamber (model MLR-350; Sanyo, Gunma, Japan).
287 The plastic bags were then removed and plants were transferred for disease development to a biosafety
288 greenhouse and incubated under a daily temperature range from 15 - 25°C, 70 - 80% RH and natural
289 photoperiod for 21 days. Weather parameters inside the biosafety greenhouse were monitored with a datalogger
290 (CR10X, Campbell Scientific Ltd., UK) connected to combined temperature-relative humidity (model
291 HMP35C) and leaf wetness (model 237) sensors. Three replicates of five plants were used in each of two
292 independent experiments.

293 Disease severity was assessed 7, 14 and 21 days after inoculation in the five youngest completely developed
294 leaves at the moment of inoculation in a plant. A 0-to-5 scale severity index (I) corresponding to a leaf area
295 affected by 0, 1, 3, 6, 12 and $\geq 24\%$, respectively (Battilani et al. 1999; Garcin et al. 2011b) was used. Disease
296 severity (S) was calculated for each plant according to the formula: $S = [(\sum_{n=1}^N I_n)/N \times 5] \times 100$ where I_n is
297 the severity index in a leaf, N is the number of leaves per plant, and 5 is the maximum severity index value on
298 the scale. In order to compare the predicted and observed values, the disease severity (S) was standardized by

299 dividing by 100 (y). CDD was calculated as the sum of the daily mean temperature in the greenhouse for the 7,
300 14 and 21 days of plant incubation, corresponding to days when the disease was assessed. A linear regression
301 analysis between predicted and observed disease severity values at each CDD was performed. The linear
302 regression was analyzed using the coefficient of determination (R^2) and testing the significance of the difference
303 in the intercept from 0 and the slope from 1.

304

305 **Results**

306 **Effect of temperature on epiphytic growth of *X. arboricola* pv. *pruni* on *Prunus* leaves under high RH**

307 The mean initial population density of *X. arboricola* pv. *pruni* strain CFBP 5563 Rif^r on inoculated leaves of
308 peach-almond hybrid GF-677, recovered after inoculation (t = 0 h), was 1.33×10^4 CFU/g. The dynamics of
309 bacterial population densities on leaf surface depended on the temperature and incubation period. The pathogen
310 was able to grow epiphytically on GF-677 leaves at temperatures from 20 to 30°C. At these temperatures no
311 increase in the bacterial population was observed in the first 12 to 24 h of incubation, but after 24 h bacterial
312 densities increased with time up to mean population densities ranging from 2.64×10^6 to 5.22×10^8 CFU/g 6-8
313 days after inoculation. In contrast, no increase in pathogen population was observed on leaves incubated at
314 temperatures from 5 to 15°C and 35°C. The epiphytic pathogen population density on leaves incubated at 35°C
315 was reduced to $< 10^2$ CFU/g after 6 days incubation under wetness. Similarly, the initial population was reduced
316 by 1-2 log units on leaves incubated at 10 and 15°C. No viable bacterial cells were recovered from leaves
317 corresponding to the negative control.

318 Population densities were used to generate the growth curves of *X. arboricola* pv. *pruni* strain CFBP 5563 Rif^r
319 on *Prunus* at each temperature. Three growth curves were obtained per temperature and experiment. The
320 modified Gompertz model (equation 1) was fitted to the growth curves obtained at temperatures at which
321 bacterial growth was observed, corresponding to 20, 25 and 30°C, and the maximum specific growth rate (μ_{\max})
322 was estimated. The doubling time ($DT = \ln(2) / \mu_{\max}$) was calculated. No significant effect of experiment
323 replicate in growth rate was observed ($P = 0.545$). Mean values for the maximum specific growth rate and the
324 doubling time at each temperature are given in Table 1. The maximum specific growth rate ranged from 0.073
325 to 0.141 h^{-1} , depending on temperature, and was higher (up to the double) at 25°C than at 20 and 30°C.
326 However, no significant differences in growth rate ($P = 0.419$) were observed between these temperatures
327 (Table 1). The mean doubling time was low (4.9 h) at 25°C and higher at 30 and 20°C (7.2 and 9.5 h,
328 respectively).

329

330 **Effect of low RH on epiphytic population dynamics of *X. arboricola* pv. *pruni* on *Prunus* leaves**

331 The mean initial population density of *X. arboricola* pv. *pruni* strain CFBP 5563 Rif^r on nectarine cv. Big Top
332 leaves was 3.9×10^8 CFU/g. Viable cell counts of pathogen recovered from the surface of 'Big Top' leaves at
333 each sampling time (from 0 to 72 h incubation at 25°C) were plotted against time to obtain the survival curves.
334 Pathogen epiphytic populations decreased with time when incubated at 25°C under dry conditions (RH < 40%)
335 (Fig. 1). During the incubation period under dry conditions, 'Big Top' leaves became flaccid and finally
336 desiccated. The survival curve for *X. arboricola* pv. *pruni* had a biphasic shape, with a rapid decline of pathogen
337 population densities at the beginning of the dry period followed by a tail in which the population density
338 maintained low. No significant differences were observed in bacterial population densities in experiment
339 replicates according to GLM analysis ($P = 0.846$), and data of three independent experiments were pooled for
340 modeling, to reduce data variability. The Cerf model (equation 2) fitted well to data (RMSE = 0.251 and $R^2 =$
341 0.931), with the following equation: $N_t = 8.59 \times [0.173 \times \exp(-0.360t)] + (1 - 0.173) \times \exp(-0.003t)$
342 (Fig. 1). The first straight phase of the curve had a negative slope (k_1) corresponding to a death rate of -0.360 log
343 CFU/g h. After 6 h incubation under dry conditions, a 2-log reduction was observed in the bacterial population
344 density, which meant that less than 10% initial cells survived. The second phase of the model (tail), had a low
345 slope ($k_2 = -0.003$ log CFU/g h), with a 1-log the reduction of bacterial epiphytic population density, slower than
346 in the first phase, in the following 66 h exposure to dry conditions. Although the reduction in the pathogen
347 population density on nectarine leaves was significant, with only 0.001% of cells surviving after 72 h incubation
348 at 25°C and low RH, not all cells were inactivated and approximately 10^6 CFU/g were recovered at the end of
349 the incubation period.

350

351 **Effect of inoculum density of *X. arboricola* pv. *pruni* on disease severity on *Prunus* leaves**

352 Two independent experiments were performed to evaluate the effects of bacterial concentration on infection and
353 disease severity on detached nectarine leaves inoculated by three different methods. Analysis of variance
354 indicated a significant effect of inoculum density and inoculation method on disease severity ($P < 0.001$), but no
355 significant effect of experiment ($P > 0.110$), so data from the two independent experiments were pooled for
356 further analysis. The effect of inoculum dose on disease severity was similar for the three inoculation methods
357 (immersion, infiltration and drop deposition), although the disease severity differed (Fig. 2). Low disease
358 severity (< 33%) was observed on leaves inoculated with densities ranging from 10^1 to 10^5 CFU/ml, whatever

359 the inoculation method. Higher inoculum concentrations, from 10^6 to 10^9 CFU/ml, resulted in significantly
360 higher disease severity (from 45 to 100% depending on the inoculation method). The local infiltration of
361 bacterial suspensions at concentrations from 10^6 to 10^9 CFU/ml produced the highest disease severity (80-
362 100%). For this method of inoculation, Tukey's HSD test separated inoculum concentrations into three groups
363 from 10^1 to 10^5 , 10^6 and higher than 10^6 CFU/ml resulting in low ($S < 45\%$), high ($S = 80\%$) and very high ($S =$
364 100%) disease severity (Fig. 2). Drop deposition of bacterial suspensions on leaf surface gave the lowest
365 severity levels: 1-20% at inoculum densities from 10^1 to 10^5 and 50-70% at higher inoculum concentrations. A
366 similar dose-response effect was observed in leaves treated by immersion in bacterial suspensions, but the
367 disease severity was slightly higher, 10-30% for low and 60-80% for high inoculum densities. Tukey's HSD test
368 for immersion and drop inoculation methods grouped inoculum densities in two groups with significantly
369 different disease severity levels: one low (10^1 - 10^5 CFU/ml) and the other high (10^6 - 10^9 CFU/ml) (Fig. 2).

370

371 **Effect of temperature and inoculum density on disease progress and symptom development**

372 Disease progress curves of two independent experiments for each temperature-inoculum density combination
373 are shown in Fig. 3. Infections occurred at temperatures from 15 to 35°C, whereas no disease symptoms were
374 observed at 10°C for any inoculum density tested. For densities of 10^6 and 10^8 CFU/ml, when the temperature
375 was increased from 15 to 30°C the disease severity also increased. A temperature of 30°C was optimal for
376 disease development, since the symptoms appeared earlier than at other temperatures with inoculum densities of
377 10^6 and 10^8 CFU/ml, and higher disease severity was reached 21 days after inoculation (Table 2, Fig. 3). The
378 minimum temperature at which symptoms were observed was 15°C, but low disease severity (12.5%) was
379 obtained with the highest inoculum concentration (10^8 CFU/ml), the final disease severity of 10^6 CFU/ml was
380 very low (0.8%), and no disease symptoms were observed at 10^4 CFU/ml. Leaves inoculated with bacterial
381 suspensions of 10^6 and 10^8 CFU/ml and incubated at 35°C also developed low disease severity. In general,
382 disease incubation period decreased and final disease severity increased when increasing the inoculum density at
383 optimal temperatures (from 20 to 30°C) (Fig. 3 and Table 2), whereas the lowest inoculum density (10^4 CFU/ml)
384 gave the lowest final disease severity and the longest incubation period (16-18 days).

385 The analysis of variance indicated no significant effect of experiment replicate ($P = 0.072$), but a significant
386 effect of temperature and inoculum density ($P < 0.001$) on disease-related parameters; incubation period, final
387 disease severity and SAUDPC. The Tukey HSD mean comparison was performed for each inoculum density
388 and disease-related parameter (Table 2). SAUDPC was significantly higher in nectarine leaves incubated at

389 30°C than in those incubated at other temperatures, whatever the inoculum density. Similar SAUDPC values
390 were observed in leaves incubated at 15, 20, 25 and 35°C and inoculated with bacterial suspensions of 10^4 (from
391 0.2 to 1.6) and 10^6 CFU/ml (from 0.3 to 4.6). However, for inoculum densities of 10^8 CFU/ml differences in
392 SAUDPC were observed with temperature, being low at 15°C (2.48), medium at 20 and 35°C (26.1 and 19.3,
393 respectively) and high at 25 and 30°C (41.5 and 60.9, respectively) (Table 2). No significant differences were
394 observed among temperatures in the incubation period at inoculum concentrations of 10^4 and 10^6 CFU/ml;
395 whereas for 10^8 CFU/ml, incubation at 25 and 30°C gave the shortest incubation period (7.7 and 5.9 days
396 respectively) and incubation at 15, 20 and 35°C resulted in longer incubation periods, from 11- 14 days (Table
397 2).

398 To obtain the symptom development model, the measure of accumulated heat (physiological time) was used,
399 expressed in CDD and calculated as the sum of daily mean temperature for a given time period with a threshold
400 temperature of 0°C. Temperatures from 20 to 30°C and the inoculum density of 10^8 CFU/ml were the most
401 favorable for symptom development according to the SAUPCD, and when disease severity was plotted against
402 CDD disease progress curves overlapped (Fig. 4). Consequently, data from treatments with inoculum density of
403 10^8 CFU/ml and 20, 25 and 30°C temperatures were used for symptom model development. The reason for
404 discarding the curves obtained at 15°C was that, after 21 days of incubation, only 315 CDD were accumulated at
405 15°C in comparison to the 420, 525 and 630 CDD at 20, 25 and 30°C, respectively (Fig. 4c and 4f); although the
406 incubation period at 15 and 20°C did not differ. For disease severity, no significant differences were observed
407 between experiments ($P = 0.184$) and temperatures ($P = 0.105$) for inoculum density of 10^8 CFU/. So, data from
408 the two experiments and the three temperatures were pooled to analyze the relationship between the disease
409 progress and the CDD (Fig. 5). The linearized form of the monomolecular, exponential, logistic and Gompertz
410 models (Table 3) were fitted to transformed severity data (z). The best model fit was obtained using the
411 linearized form of the Gompertz model ($R^2 = 0.715$, $MSE = 0.511$ and $R^{2*} = 0.778$), with parameter estimates b_0
412 = -2.7869 and $r_G = 0.0112$. Parameter b_0 and values predicted by the linear model (z) were back-transformed to
413 the original equation of Gompertz using: $B = \exp(-b_0)$ and $y = \exp[-\exp(-z)]$. The Gompertz equation describes
414 the S-shaped curve of the dependent variable over CDD: $y = \exp [-B \cdot \exp(-r_G \cdot CDD)]$, where y is the disease
415 severity (0-1); B is a constant of integration ($-\ln(y_0)$) and r_G is the slope. According to the obtained Gompertz
416 model, 281.6 CDD were necessary for a disease severity of 50%, while 150 and 174 CDD were necessary to
417 reach 5 and 10% disease severity, respectively.

418 The predictive capacity of the symptom development model was evaluated in two additional experiments, in
419 which *Prunus* plants were inoculated with bacterial suspensions containing 1×10^8 CFU/ml, exposed for 24 h at
420 25°C under wetness to induce infection, and then, incubated in the greenhouse for symptom development at a
421 daily temperature range of 15-25°C. Disease severity was assessed 7, 14 and 21 days after inoculation and the
422 corresponding CDD was calculated. Observed disease severity and disease severity predicted by the Gompertz
423 model at each CDD were compared. A significant correlation was obtained between observed and predicted
424 values of disease severity ($P < 0.01$), with a Pearson coefficient $R = 0.909$. The linear regression of the predicted
425 against the observed disease severity is shown in Fig. 6, with a coefficient of determination $R^2 = 0.83$ and the
426 intercept and the slope not significantly different from 0 ($P = 0.963$) and 1 ($P = 0.815$), respectively.

427

428 **Discussion**

429 A better understanding of bacterial spot disease epidemiology can be valuable in developing disease
430 management strategies based on the use of disease forecasters in decision support systems to guide copper
431 applications and disease surveillance tasks for early detection of outbreaks or spread of the disease. This study
432 contributes to increase the knowledge on some epidemiological aspects of the bacterial spot disease of stone
433 fruits and provides new information that will be the basis for the development of a forecasting system for this
434 disease.

435 Epiphytic growth of *X. arboricola* pv. *pruni* on *Prunus* leaves was only observed at temperatures of 20, 25 and
436 30°C, being maximal at 25°C. In previous *in vitro* studies, the bacterium was able to grow at temperatures from
437 5 to 35°C, with a maximum at 30°C (Morales et al. 2017). As expected, the maximum specific growth rate and
438 the doubling time for the epiphytic growth of *X. arboricola* pv. *pruni* on *Prunus* leaves differed from those
439 determined *in vitro*. For a given temperature, the maximum specific growth rate for strain CFBP 5563 on
440 *Prunus* leaves was lower than that obtained for the same strain when grown *in vitro*, in LB broth. These
441 differences can be attributed to the growth conditions, mainly nutrient and free water availability. The growth of
442 epiphytic bacteria on plant surface is limited by the availability of nutrients, and the lack of carbon sources on
443 the leaf surface has been reported (Mercier and Lindow 2000). Additionally, only a few sites on the leaf surface,
444 such as veins and trichomes, offer conditions that allow bacterial growth. These specific sites protect bacteria
445 from water stress since they retain water longer than other parts, which may increase the local availability of
446 nutrients such as sugars, which are used by bacteria on the leaf surface (van der Wal et al. 2013). Consequently,
447 although the pathogen was initially uniformly distributed onto the leaf surface by leaf immersion in the bacterial

448 suspension, only specific areas were colonized by the bacterium. In contrast, *X. arboricola* pv. *pruni* growth *in*
449 *vitro* was not limited by nutrients or free water since LB broth is a nutritionally rich medium with high water
450 activity ($a_w = 0.975$). Detached leaves appear to be a useful approach for analyzing the potential epiphytic
451 bacterial growth since they more closely reflect natural conditions, with limited carbon sources, a reduction of
452 water activity, and interaction with host factors (Lebeaux et al. 2013). However, it should be taken into account
453 that, under natural conditions, phyllosphere microbial communities are diverse and their diversity and
454 population size are influenced by environmental conditions and host factors (plant species, plant cultivar, and
455 stage of growth) (Gnanamanickam and Immanuel 2007). Consequently, diversity of microbial communities
456 present in the phylloplane may affect host colonization by epiphytic populations of *X. arboricola* pv. *pruni*.
457 Information obtained in this study could be combined with the model for predicting *X. arboricola* pv. *pruni*
458 growth as a function of temperature developed under *in vitro* conditions and used to forecast the inoculum
459 potential for this pathogen.

460 Although bacterial growth is a temperature-dependent process, it requires the presence of free water, provided
461 by rain, dew or irrigation, a situation that does not always occur on host tissues under field conditions (Agrios
462 2005; Garcin et al. 2007; Moh et al. 2011). The multiplication of the pathogen, as well as the infection process,
463 may be interrupted by a dry period (Magarey and Sutton, 2007). In this research, variations in the density of *X.*
464 *arboricola* pv. *pruni* epiphytic populations under different wetness conditions were analyzed. The population
465 density on *Prunus* leaves decreased when incubated under low RH (< 40%) at optimal temperature for growth
466 (25°C) in contrast to the population increase observed under wetness. The survival curve under dry conditions
467 contained two separate phases, a rapid decline of population during the first 6 h of dryness followed by a slow
468 and continuous inactivation of bacterial cells on increasing the dry period. Similar results were observed in
469 experiments with lower initial bacterial concentrations (10^6 CFU/ml); a biphasic curve with the turning point
470 after 6 h of dryness was also obtained (data not shown). Accordingly, 6 h may be the time required for *X.*
471 *arboricola* pv. *pruni* to activate the mechanisms to respond and adapt to dry conditions. The presence of these
472 two phases has been considered to represent a mix of two fractions or sub-populations of different head
473 resistance, in which the first phase describes the inactivation of the less resistant cells and the second phase
474 corresponds to the more resistant ones (Xiong et al. 1999). *Xanthomonads* are able to synthesize large amounts
475 of lipopolysaccharides and the extracellular polysaccharide xanthan. The abundant xanthan slime layer aids in
476 bacterial adhesion with biofilm formation, survival and infection (Crossman and Dow 2004; Ryan et al. 2011;
477 Schubert et al. 2001), and probably protects against dehydration, which could explain the survival of 0.001%

478 bacterial population after 72 h incubation under low RH. A combined model for predicting the epiphytic
479 inoculum potential of *X. arboricola* pv. *pruni* based on temperature and wet/dry periods could be developed by
480 integrating results obtained here and in previous studies (Morales et al. 2017), in a similar way to *X. campestris*
481 pv. *vesicatoria* (Kim et al. 2014) and *Pseudomonas syringae* pv. *actinidiae* (Beresford et al. 2017) prediction
482 models.

483 The relationship between inoculum density and infection of *Prunus* by *X. arboricola* pv. *pruni* was determined
484 on detached leaf assays using three inoculation methods. All inoculation methods were effective for bacterial
485 infection and disease symptom development despite quantitative variance in disease expression. Leaves
486 inoculated by infiltration expressed the highest disease severity, explained by the fact that bacterial cells were
487 introduced directly into the leaf mesophyll. Although the severity was lower in leaves inoculated by immersion
488 or drop deposition, these methods may reflect natural infections more accurately because bacterial cells had to
489 enter leaves through natural openings or wounds (Battilani et al. 1999; Garcin et al. 2011a; Morales et al. 2016,
490 2017). Nevertheless, a similar pattern of the effect of inoculum dose on disease severity was observed for the
491 three inoculation methods. Low severity obtained at inoculum densities below 10^6 CFU/ml and high disease
492 severity recorded at inoculum densities from 10^6 to 10^9 CFU/ml agreed with previous reports (Civerolo 1975;
493 Socquet-Juglard et al. 2012) and could be related to quorum sensing. Several regulatory systems depend on
494 quorum sensing mechanisms, widely studied for *X. campestris* (Dow et al., 2003; He and Zhang, 2008),
495 whereby bacteria monitor their local population density before expressing a phenotype or to control
496 pathogenicity genes (von Bodman et al. 2003; Whitehead et al. 2001). Supporting this idea, *X. arboricola* pv.
497 *pruni* has been detected on symptomless peach twigs over a year with a maximum of 6.1×10^4 CFU/g of fresh
498 weight (Shepard and Zehr 1994), and from 10^2 to 10^5 CFU/ml bacterial densities have been detected in
499 asymptomatic leaves of *Prunus* field samples, whereas at least 10^6 CFU/ml were present in symptomatic leaves
500 (Palacio-Bielsa et al. 2011). Our results confirm that 10^6 CFU/ml can be considered the minimum concentration
501 for *X. arboricola* pv. *pruni* to cause infections, and seems to be the threshold for bacterial cells to activate
502 pathogenesis on host leaves and change from the epiphytic phase through an endophytic phase. Additionally, the
503 inoculum density was also related to the incubation time, since longer incubation periods and lower final disease
504 severity values were observed in leaves inoculated with doses below 10^6 CFU/ml.

505 Once infections occur, temperature is probably the major conditioning factor for disease progress and symptom
506 development, but it also depends on the specific host-pathogen combination (Agrios 2005; Dickson and Holbert
507 1928). In our study, disease progress and symptom development were observed at temperatures from 15 to

508 35°C, with the optimum at 30°C, which agree with the optimal temperatures for the pathogen growth (Morales et
509 al. 2017; Young et al. 1977). The cumulative degree day, CDD, as predictor of the physiological time, has been
510 used to forecast symptom development in plant disease forecasting models, such as Maryblyt (Lightner and
511 Steiner 1992) and BIS95 (Billing 1999). The same concept was applied in our study to predict symptom
512 development of bacterial spot disease of stone fruits. The relationship between the progress of disease severity
513 and CDD was described by the Gompertz model, whereby 150, 175 and 280 CDD with a temperature base of
514 0°C were required for disease severity of 5, 10 and 50%, respectively. The biofix to initiate the computation of
515 CDD is the date when infections occur. An incubation period of 250 CDD (with a threshold temperature of
516 10.8°C) had been determined for bacterial spot disease of stone fruits in a previous study performed under field
517 conditions, in French peach orchards naturally affected by the disease (Garcin et al. 2011b). Symptom
518 development under field conditions may be affected by temperature, but also by other weather variables, such as
519 leaf wetness or RH (Zehr et al. 1996), as well as the inoculum density of natural pathogen populations
520 (Randhawa and Civerolo 1985). The incubation period for bacterial spot disease reported on Italian peach
521 orchards varied from 6 to 26 days in warm and cold weather, respectively (Battilani et al. 1999). Variation on
522 the CDD found in our study and those performed under natural conditions may be partially attributed to
523 pathogen inoculum density, which was probably lower in the orchards than in our experiments performed under
524 controlled conditions (10^8 CFU/ml). The model for predicting the incubation period developed and validated in
525 the work presented here needs to be evaluated under field conditions before its practical application.

526 The information generated in this study, performed under controlled environment and greenhouse conditions,
527 will be useful in the development of a disease forecasting system for *X. arboricola* pv. *pruni*. Our approach for
528 the development of a forecaster for bacterial spot disease of stone fruits was focused on three crucial stages of
529 the disease cycle: host colonization by epiphytic populations of the pathogen, host infection and disease
530 progress and symptom development. Consequently, the forecasting system will be composed of three
531 components: i) the epiphytic inoculum potential, ii) the infection model and, iii) the disease symptom
532 development model. The first component of the forecasting system, which refers to pathogen potential
533 inoculum, will be based on the model for *X. arboricola* pv. *pruni* growth *in vitro* as a function of temperature
534 (Morales et al. 2017) and the results of epiphytic growth under wet/dry periods from this study. The relationship
535 between the inoculum dose of *X. arboricola* pv. *pruni* and the onset of the infection process is an essential
536 parameter for operation of the forecasting system, since it links the epiphytic inoculum potential with the
537 infection model. The infection threshold of 10^6 CFU/ml should be included in the forecasting system to link the

538 epiphytic inoculum potential and the infection model. Therefore, the infection model (second component)
539 developed and validated previously (Morales et al. 2018) will start working when the inoculum potential
540 predicted by the growth model is high enough to cause infections. Therefore, if the infection model predicts
541 favorable weather conditions for initiating an infection process, the symptom model will run for prediction of
542 disease symptoms appearance on the basis of daily mean temperature and CDD. The whole forecasting system
543 proposed needs to be evaluated under field conditions in experimental or commercial orchards before being used
544 in decision support systems (DSS) for management of the bacterial spot disease of stone fruits.

545

546 **Compliance with Ethical Standards**

547 This research was supported, in part, by grants from the Ministerio de Educación, Ciencia y Deporte (AGL2013-
548 41405-R) of Spain, from the University of Girona (SING12/13 and MPCUdG2016/085) and from the European
549 Union's Seventh Framework Programme for research, technological development and demonstration under grant
550 agreement number 613678 (DROPSA). Gerard Morales was the recipient of predocotoral fellowships from the
551 University of Girona (BR 2013/31) and from MECED (FPU13/04123) from Spain.

552 The authors declare that they have no conflict of interest.

553

554 **Acknowledgements**

555 We are grateful to Agromillora Catalana for supplying plant material (GF677 plants). We thank Marc Nicolàs
556 and Josep Pereda for helpful collaboration, and Shirley Burgess for assistance in language editing.

557

558 **Literature cited**

559 Agrios, G. N. (2005). *Plant Pathology* (5th edition). San Diego, California: Elsevier Academic Press.

560 Anonymous. (2006) EPP0 standards PM7/64. Diagnostics protocols for regulated pests. *Xanthomonas*
561 *arboricola* pv. *pruni*. *Bulletin OEPP/EPPO Bulletin*, 36: 129–133.

562 Battilani, P., Rossi, V., & Saccardi, A. (1999). Development of *Xanthomonas arboricola* pv. *pruni* epidemics on
563 peaches. *Journal of Plant Pathology*, 81(3), 161–171.

564 Baty, F., Ritz, C., Charles, S., Brutsche, M., Flandrois, J. P., & Delignette-Muller M. L. (2015). A toolbox for
565 nonlinear regression in R: the package nlstools. *Journal of Statistical Software*, 66(5):1–21.

566 Beresford, R. M., Tyson, J. L., & Henshall, W. R. (2017). Development and validation of an infection risk
567 model for bacterial canker of kiwifruit, using a multiplication and dispersal concept for forecasting bacterial
568 diseases. *Phytopathology*, 107(2), 184–191.

569 Billing, E. (1984). Principles and applications of fire blight risk assessment systems. *Acta Horticulturae*, 151,
570 15–22.

571 Billing, E. (1999). Fire blight risk assessment: Billing’s integrated system (BIS) and its evaluation. *Acta*
572 *Horticulturae*, 489, 399–406.

573 Boudon, S., Manceau, C., & Nottéghem, J. L. (2005). Structure and origin of *Xanthomonas arboricola* pv. *pruni*
574 populations causing bacterial spot of stone fruit trees in western Europe. *Phytopathology*, 95(9), 1081–1088.

575 Campbell, C., & Madden, L. (1990). *Introduction to Plant Disease Epidemiology*. New York: Wiley.

576 Cerf, O. (1977). Tailing of survival curves of bacterial spores. *Journal of Applied Bacteriology*, 42(1), 1–19.

577 Civerolo, E. (1975). Quantitative aspects of pathogenesis of *Xanthomonas pruni* in peach leaves.
578 *Phytopathology*, 65, 258–264.

579 Crossman, L., & Dow, J. M. (2004). Biofilm formation and dispersal in *Xanthomonas campestris*. *Microbes and*
580 *Infection*, 6, 623–629.

581 Dickson, J., & Holbert, J. (1928). The relation of temperature to the development of disease in plants. *The*
582 *American Naturalist*, 62(681), 311–333.

583 Dhingra, O. D., & Sinclair, J. B. (1985) *Basic Plant Pathology Methods* (2nd edition). Boca Raton, FL: CRC
584 Press.

585 Dow, J. M., Crossman, L., Findlay, K., He, Y. Q., Feng, J. X., & Tang, J. L. (2003). Biofilm dispersal in
586 *Xanthomonas campestris* is controlled by cell-cell signaling and is required for full virulence to plants.
587 *Proceedings of the National Academy of Sciences*, 100(19), 10995–11000.

588 EFSA Panel on Plant Health. (2014). Scientific opinion on pest categorisation of *Xanthomonas arboricola* pv.
589 *pruni* (Smith, 1903). *EFSA Journal*, 12(10), 3857–3882.

590 EPPO. (2017). *Xanthomonas arboricola* pv. *pruni* (XANTPR). EPPO Global Database. Retrieved from
591 <https://gd.eppo.int>.

592 EPPO/CABI. (1997). *Xanthomonas arboricola* pv. *pruni*. In Smith I. M., McNamara D. G., Scott P. R., &
593 Holderness M. (Eds.), *Quarantine Pests for Europe* (2nd ed., pp. 1096–1100). Wallingford, UK: CAB
594 International.

595 Garcin, A., Neyrand, S., & Fabresse, M. (2007). Fruits á noyau: Sensibilité variétale au *Xanthomonas*.
596 *L'arboriculture fruitière*, 612, 28–32.

597 Garcin, A., Vibert, J., & Cellier, M. (2011a). *Xanthomonas* sur pêcher: étude des conditions d'infection.
598 Fonctionnement du modèle et résultats d'essais (2e partie). *Infos CTIFL*, 272, 30–39.

599 Garcin, A., Vibert, J., & Leclerc, A. (2011b). *Xanthomonas* sur pêcher: étude des conditions d'infection.
600 Développement de l'outil (1re partie). *Infos CTIFL*, 268, 26–39.

601 Giovanardi D., Dallai D., & Stefani E. (2016). Population features of *Xanthomonas arboricola* pv. *pruni* from
602 *Prunus* spp. orchards in northern Italy. *European Journal of Plant Pathology*, 147, 761-771.

603 Gnanamanickam S. S., & Immanuel J. E. (2007) Epiphytic bacteria, their ecology and functions. In
604 Gnanamanickam S. S. (Eds.) *Plant-Associated Bacteria*. Dordrecht: Springer Netherlands.

605 Goodman, R. N. (1976). Physiological and cytological aspects of the bacterial infection process. In Heitefuss,
606 R., & Williams, P. H. (Eds.), *Physiological Plant Pathology. Encyclopedia of Plant Physiology* (New Series,
607 vol.4, pp. 172–196). Berlin: Springer.

608 He, Y. W., & Zhang, L. H. (2008). Quorum sensing and virulence regulation in *Xanthomonas campestris*.
609 *FEMS Microbiology Reviews*, 32(5), 842–857.

610 Janse, J. D. (2012). Bacterial diseases that may or do emerge, with (possible) economic damage for Europe and
611 the Mediterranean basin: Notes on epidemiology, risks, prevention and management on first occurrence.
612 *Journal of Plant Pathology*, 94(Supplement 4), S4.5-S4.29.

613 Kim, J., Kang, W., & Yun, S. (2014). Development of a model to predict the primary infection date of bacterial
614 spot (*Xanthomonas campestris* pv. *vesicatoria*) on hot pepper. *The Plant Pathology Journal*, 30(2), 125–135.

615 Lalancette, N., & McFarland, K. (2007). Phytotoxicity of copper-based bactericides to peach and nectarine.
616 *Plant Disease*, 91(9), 1122–1130.

617 Lebeaux, D., Chauhan, A., Rendueles, O., & Beloin, C. (2013). From *in vitro* to *in vivo* models of bacterial
618 biofilm-related infections. *Pathogens*, 2(2), 288–356.

619 Lightner, G. W., & Steiner, P. W. (1992). Maryblyt™: A computer model for predicting of fire blight disease in
620 apples and pears. *Computers and Electronics in Agriculture*, 7(3), 249–260.

621 Lindemann, J. (1984). Use of an apparent infection threshold population of *Pseudomonas syringae* to predict
622 incidence and severity of brown spot of bean. *Phytopathology*, 74(11), 1334–1339.

623 Magarey, R. D., & Sutton, T. B. (2007). How to create and deploy infection models for plant pathogens. In
624 Ciancio, A., & Mukerji, K. G. (Eds.), *Integrated Management of Plants Pests and Diseases* (Volume 1, pp.
625 3–25). Dordrecht: Springer Netherlands.

626 Mercier, J., & Lindow, S. E. (2000). Role of leaf surface sugars in colonization of plants by bacterial epiphytes.
627 *Applied and Environmental Microbiology*, 66(1), 369–374.

628 Moh, A., Massart, S., & Lahlali, R. (2011). Predictive modelling of the combined effect of temperature and
629 water activity on the *in vitro* growth of *Erwinia* spp. infecting potato tubers in Belgium. *Biotechnology,*
630 *Agronomy, Society and Environment*, 15(3), 379–386.

631 Moragrega, C., Manceau, C., & Montesinos, E. (1998). Evaluation of drench treatments with phosphonate
632 derivatives against *Pseudomonas syringae* pv. *syringae* on pear under controlled environment conditions.
633 *European Journal of Plant Pathology*, 104(2), 171–180.

634 Morales, G., Llorente, I., Montesinos, E., & Moragrega, C. (2016). Basis for a predictive model of *Xanthomonas*
635 *arboricola* pv. *pruni* growth and infections in host plants. *Acta Horticulturae*, 1149, 1–8.

636 Morales, G., Llorente, I., Montesinos, E., & Moragrega, C. (2017). A model for predicting *Xanthomonas*
637 *arboricola* pv. *pruni* growth as a function of temperature. *PLoS ONE*, 12(5), e0177583.
638 <https://doi.org/10.1371/journal.pone.0177583>.

639 Morales, G., Moragrega, C., Montesinos, E., & Llorente, I. (2018). Effects of leaf wetness duration and
640 temperature on infection of *Prunus* by *Xanthomonas arboricola* pv. *pruni*. *PLoS ONE* 13(3): e0193813.
641 <https://doi.org/10.1371/journal.pone.0193813>.

642 Palacio-Bielsa, A., Cubero, J., Cambra, M. a, Collados, R., Berruete, I. M., & Lopez, M. M. (2011).
643 Development of an efficient real-time quantitative PCR protocol for detection of *Xanthomonas arboricola*
644 pv. *pruni* in *Prunus* species. *Applied and Environmental Microbiology*, 77(1), 89–97.

645 Palacio-Bielsa, A., Roselló, M., Cambra, M. A., & López, M. M. (2010). First report on almond in Europe of
646 bacterial spot disease of stone fruits caused by *Xanthomonas arboricola* pv. *pruni*. *Plant Disease*, 94(6),
647 786.

648 Randhawa, P. S., & Civerolo, E. (1985). A detached-leaf bioassay for *Xanthomonas campestris* pv. *pruni*.
649 *Phytopathology*, 75(9), 1060–1063.

650 Ritchie, D. F. (1995). Bacterial spot. In: Ogawa J. M., Zehr E. I., Bird G. W., Ritchie D. F., Uriu, K., &
651 Uyemoto, J. K. (Ed.) *Compendium of Stone Fruit Diseases*. St. Paul: APS Press.

652 Ritchie, D. F. (2004). Copper-containing fungicides/bactericides and their use in management of bacterial spot
653 on peaches. *Southeast Regional Newsletter*, 4(1).

654 Ruz, L., Moragrega, C., & Montesinos, E. (2008). Evaluation of four whole-plant inoculation methods to
655 analyze the pathogenicity of *Erwinia amylovora* under quarantine conditions. *International*
656 *Microbiology*, 11(2), 111–119.

657 Ryan, R. P., Vorhölter, F.-J., Potnis, N., Jones, J. B., Van Sluys, M.-A., Bogdanove, A. J., & Dow, J. M. (2011).
658 Pathogenomics of *Xanthomonas*: understanding bacterium-plant interactions. *Nature Reviews Microbiology*,
659 9(5), 344–355.

660 Schubert, T., Rizvi, S., Sun, X., Gottwald, T., Graham, J., & Dixon, W. (2001). Meeting the challenge of
661 eradicating citrus canker in Florida - again. *Plant Disease*, 85(4), 340–356.

662 Scortichini, M. (2010). Epidemiology and predisposing factors of some major bacterial diseases of stone and nut
663 fruit trees species. *Journal of Plant Pathology*, 92(Supplement 1), S1.73-S1.78.

664 Shepard, D., & Zehr, E. (1994). Epiphytic persistence of *Xanthomonas campestris* pv. *pruni* on peach and plum.
665 *Plant Disease*, 78(6), 627–629.

666 Smith, E. (1903). Observation on a hitherto unreported bacterial disease the cause of which enters the plant
667 through ordinary stomata. *Science*, 17, 456–457.

668 Smith, T. (1993). A predictive model for forecasting fire blight of pear and apple in Washington State. *Acta*
669 *Horticulturae*, 338, 153–160.

670 Socquet-Juglard, D., Patocchi, A., Pothier, J. F., Christen, D., & Duffy, B. (2012). Evaluation of *Xanthomonas*
671 *arboricola* pv. *pruni* inoculation techniques to screen for bacterial spot resistance in peach and apricot.
672 *Journal of Plant Pathology*, 94(Supplement 1), S1.91-S1.96.

673 Stefani, E. (2010). Economic significance and control of bacterial spot/canker of stone fruits caused by
674 *Xanthomonas arboricola* pv. *pruni*. *Journal of Plant Pathology*, 92(Supplement 1), 99–104.

675 Stockwell, V. O., & Duffy, B. (2012). Use of antibiotics in plant agriculture. *Scientific and Technical Review of*
676 *the Office International des Epizooties*, 31(1), 199–210.

677 van der Wal, A., Tecon, R., Kreft, J.-U., Mooij, W. M., & Leveau, J. H. J. (2013). Explaining bacterial
678 dispersion on leaf surfaces with an individual-based model (PHYLLOSIM). *PLoS ONE*, 8(10), e75633.
679 <https://doi.org/10.1371/journal.pone.0075633>.

680 Vanneste, J., McLaren, G., & Yu, J. (2005). Copper and streptomycin resistance in bacterial strains isolated
681 from stone fruit orchards in New Zealand. *New Zealand Plant Protection*, 58, 101–105.

682 Vauterin, L., Hoste, B., Kersters, K., & Swings, J. (1995). Reclassification of *Xanthomonas*. *International*
683 *Journal of Systematic Bacteriology*, 45(3), 472–489.

684 von Bodman, S. B., Bauer, W. D., & Coplin, D. L. (2003). Quorum sensing in plant-pathogenic bacteria. *Annual*
685 *Review of Phytopathology*, 41, 455–82.

686 Wert, T. W., Miller, P., Williamson, J. G., & Rouse, R. E. (2006). Preliminary studies for controlling bacterial
687 spot in low-chill peaches. *Proceedings of the Florida State Horticultural Society*, 119, 32–33.

688 Whitehead, N. A., Barnard, A. M. L., Slater, H., Simpson, N. J. L., & Salmond, G. P. C. (2001). Quorum-
689 sensing in Gram-negative bacteria. *FEMS Microbiology Reviews*, 25(4), 365–404.

690 Xiong, R., Xie, G., Edmondson, A. E., & Sheard, M. A. (1999). A mathematical model for bacterial
691 inactivation. *International Journal of Food Microbiology*, 46(1), 45–55.

692 Young, J., Luketina, R., & Marshall, A. (1977). The effects on temperature on growth *in vitro* of *Pseudomonas*
693 *syringae* and *Xanthomonas pruni*. *Journal of Applied Bacteriology*, 42(3), 345–354.

694 Zehr, E. I., Shepard, D. P., & Bridges Jr, W. C. (1996). Bacterial spot of peach as influenced by water
695 congestion, leaf wetness duration, and temperature. *Plant Disease*, 80(3), 339–341.

696 Zwietering, M., Jongenburger, I., Rombouts, F. M., & van't Riet, K. (1990). Modeling of the bacterial growth
697 curve. *Applied and Environmental Microbiology*, 56(6), 1875–1881.

698

699 **Tables**

700 Table 1 Growth parameters estimated by the modified Gompertz model for epiphytic populations of *X.*
 701 *arboricola* pv. *pruni* on *Prunus* leaves at different temperatures under high RH

Temperature (°C)	Maximum specific growth rate (h ⁻¹) ^y	Doubling time (h) ^y
5	- ^z	-
10	-	-
15	-	-
20	0.073 ± 0.027	9.54 ± 3.6
25	0.141 ± 0.034	4.92 ± 1.2
30	0.099 ± 0.033	7.02 ± 2.3
35	-	-

702 ^y Maximum specific growth rate (μ_{max}) was estimated from the modified Gompertz model fitted to
 703 growth curves at different temperatures. Doubling time = $\ln(2) / \mu_{max}$. Values are the mean of
 704 two experiments.

705 ^z:- no growth was observed.

706

707 Table 2 Effect of temperature (T) and inoculum density (ID) on bacterial spot disease development on *Prunus*
 708 leaves inoculated with *X. arboricola* pv. *pruni*

ID (CFU/ml)	T (°C)	Disease development parameters ^w		
		Disease severity (%) ^x	SAUDPC ^y	Incubation period (days)
10 ⁴	10	- ^z	-	-
	15	-	-	-
	20	7.5 ± 5.0 b	1.01 ± 0.69 b	18.0 ± 1.0 a
	25	5.8 ± 2.8 b	1.57 ± 0.95 b	16.3 ± 1.7 a
	30	27.5 ± 9.0 a	6.29 ± 2.26 a	17.0 ± 1.0 a
	35	1.7 ± 1.7 b	0.20 ± 0.20 b	18.0 ± 7.5 a
	10 ⁶	10	-	-
15		0.8 ± 0.8 C	0.30 ± 0.30 B	14.0 ± 0.0 A
20		20.0 ± 5.2 BC	2.38 ± 1.07 B	15.8 ± 2.7 A
25		23.3 ± 6.1 B	4.44 ± 1.61 B	12.4 ± 3.0 A
30		81.7 ± 8.9 A	28.77 ± 4.16 A	10.8 ± 0.5 A
35		15.0 ± 5.4 BC	4.56 ± 1.65 B	12.4 ± 0.2 A
10 ⁸		10	-	-
	15	12.5 ± 4.5 C'	2.48 ± 1.27 D'	14.1 ± 1.9 A'
	20	98.3 ± 1.1 A'	26.11 ± 2.36 C'	12.2 ± 0.9 A'B'
	25	93.3 ± 3.7 A'	41.67 ± 4.65 B'	7.7 ± 0.7 C'
	30	100.0 ± 0.0 A'	60.95 ± 1.45 A'	5.9 ± 0.2 C'
	35	47.5 ± 13.2 B'	19.35 ± 5.91 C'	11.7 ± 1.1 B'

709 ^w Values are the mean of two experiments, with five leaf-replicates per temperature-inoculum
 710 density combination and experiment. For each ID means followed by the same letter did not
 711 differ significantly ($P = 0.05$) according to the Tukey's HDS mean comparison test.

712 ^x Disease severity at the end of incubation period (21 days after inoculation).

713 ^y SAUDPC: Standardized area under the disease progress curve (AUDPC divided by the length
 714 of incubation; 21 days).

715 ^z -: disease symptoms were not observed.

716

717

718 Table 3 Description and parameters of models fitted to the bacterial spot disease progress curves

Model ^y	Linearized equation ^z	b_0	r	R^2	MSE	R^{2*}
Monomolecular	$\ln\left(\frac{1}{1-y}\right) = b_0 + r_M CDD$	-1.4633	0.0083	0.670	0.343	0.688
Exponential	$\ln(y) = b_0 + r_E CDD$	-3.2572	0.0074	0.545	0.462	0.538
Logistic	$\ln\left(\frac{y}{1-y}\right) = b_0 + r_L CDD$	-4.7206	0.0157	0.699	1.075	0.784
Gompertz	$-\ln[-\ln(y)] = b_0 + r_G CDD$	-2.7869	0.0112	0.715	0.511	0.778

719 ^y Models were fitted to pooled disease severity data from *Prunus* leaves inoculated with 10⁸ CFU/ml
 720 suspensions of *X. arboricola* pv. *pruni* CFBP 5563 and incubated for 21 days at 20, 25 and 30°C for
 721 disease development. Data from two independent experiments were used.

722 ^z Adapted from Campbell and Madden (1990). y : disease severity (0-1); b_0 and r : intercept and slope
 723 parameters of the linearized forms of the models; CDD : cumulative degree day; R^2 and MSE :
 724 coefficient of determination and mean square error of linear regression; R^{2*} : coefficient of
 725 determination between predicted back-transformed values and observed values.

726

727

728 **Figure captions**

729 **Fig. 1** Survival curve of epiphytic populations of *X. arboricola* pv. *pruni* strain CFBP 5563 Rif^r on nectarine cv.
730 Big Top leaves incubated for 72 h at 25°C under low HR (< 40%). Values are the mean of three five-leaf
731 replicates per sampling time for three independent experiments. Cerf model is represented with continuous line.
732 Error bar (upper right corner) corresponds to the mean standard error

733

734 **Fig. 2** Effect of inoculum density on infection of nectarine cv. Big Top leaves by *X. arboricola* pv. *pruni* using
735 three different inoculation methods: leaf immersion in the bacterial suspension (a); local infiltration of 25 µl of
736 bacterial suspension in the leaf (b), and deposition of a 25-µl drop bacterial suspension onto the leaf surface (c).
737 Bars are the mean disease severity after 21 days incubation at 25°C of two independent experiments and three
738 replicates per experiment. Error bars are the standard error. Different letters indicate significant differences
739 according to Tukey's mean separation test ($P = 0.05$)

740

741 **Fig. 3** Effect of temperature and inoculum density on bacterial spot disease development on peach-almond
742 hybrid GF-677 leaves inoculated with *X. arboricola* pv. *pruni* strain CFBP 5563. Three inoculum densities were
743 tested: 10^4 CFU/ml (a and d), 10^6 CFU/ml (b and e), and 10^8 CFU/ml (c and f). Values are the mean of five-leaf
744 replicates. Global mean standard error was ± 1.32 . The experiment was performed twice (Exp. 1 and Exp. 2)

745

746 **Fig. 4** Bacterial spot disease progress as a function of cumulative degree days (CDD) in leaves of the peach-
747 almond hybrid GF-677 inoculated with *X. arboricola* pv. *pruni* strain CFBP 5563 at different inoculum densities
748 10^4 CFU/ml (a and d), 10^6 CFU/ml (b and e), and 10^8 CFU/ml (c and f) and incubated at different temperatures.
749 The experiment was performed twice. Values are the mean disease severity of five-leaf replicates. Global mean
750 standard error was ± 1.32

751

752 **Fig. 5** Relationship between bacterial spot disease severity and cumulative degree days (°C) on peach-almond
753 hybrid GF-677 plants inoculated with *X. arboricola* pv. *pruni* strain CFBP 5563 10^8 CFU/ml and incubated
754 under controlled environment conditions at 20 (●), 25 (○) and 30°C (▲). Regression lines were calculated by
755 combining the results for the three temperatures in two independent experiments. Each data point is the mean of
756 five-leaf replicates. a, Linearized form of the Gompertz model ($z = -2.7869 + 0.0112 \cdot CDD$, $R^2 = 0.71$). b,
757 Gompertz model, back-transformed from the linearized form ($y = \exp [-16.2306 \cdot \exp(-0.0112 \cdot CDD)]$)

758
759
760
761
762
763
764
765
766
767
768
769
770

Fig. 6 Validation of the symptom development model for bacterial spot disease in potted plants of the peach-almond hybrid GF-677 inoculated with *X. arboricola* pv. *pruni* strain CFBP 5563 (10^8 CFU/ml) and incubated under greenhouse conditions for 21 days. Values are the mean disease severity of three replicates of five plants for each of two independent experiments (black and white circles). a, Gompertz model, back-transformed from the linearized form ($y = \exp [-16.2306 \cdot \exp (-0.0112 \cdot CDD)]$). b, observed disease severity versus predicted severity by the linearized form of the Gompertz model. The regression line was not different from a line with an intercept of 0 and a slope of 1

Table 1 Growth parameters estimated by the modified Gompertz model for epiphytic populations of *X. arboricola* pv. *pruni* on *Prunus* leaves at different temperatures under high RH

Temperature (°C)	Maximum specific growth rate (h ⁻¹) ^y	Doubling time (h) ^y
5	- ^z	-
10	-	-
15	-	-
20	0.073 ± 0.027	9.54 ± 3.6
25	0.141 ± 0.034	4.92 ± 1.2
30	0.099 ± 0.033	7.02 ± 2.3
35	-	-

^y Maximum specific growth rate (μ_{max}) was estimated from the modified Gompertz model fitted to growth curves at different temperatures. Doubling time = $\ln(2) / \mu_{max}$. Values are the mean of two experiments.

^z:- no growth was observed.

Table 2 Effect of temperature (T) and inoculum density (ID) on bacterial spot disease development on *Prunus* leaves inoculated with *Xanthomonas arboricola* pv. *pruni*

ID (CFU/ml)	T (°C)	Disease development parameters ^w		
		Disease severity (%) ^x	SAUDPC ^y	Incubation period (days)
10 ⁴	10	- ^z	-	-
	15	-	-	-
	20	7.5 ± 5.0 b	1.01 ± 0.69 b	18.0 ± 1.0 a
	25	5.8 ± 2.8 b	1.57 ± 0.95 b	16.3 ± 1.7 a
	30	27.5 ± 9.0 a	6.29 ± 2.26 a	17.0 ± 1.0 a
	35	1.7 ± 1.7 b	0.20 ± 0.20 b	18.0 ± 7.5 a
	10 ⁶	10	-	-
15		0.8 ± 0.8 C	0.30 ± 0.30 B	14.0 ± 0.0 A
20		20.0 ± 5.2 BC	2.38 ± 1.07 B	15.8 ± 2.7 A
25		23.3 ± 6.1 B	4.44 ± 1.61 B	12.4 ± 3.0 A
30		81.7 ± 8.9 A	28.77 ± 4.16 A	10.8 ± 0.5 A
35		15.0 ± 5.4 BC	4.56 ± 1.65 B	12.4 ± 0.2 A
10 ⁸		10	-	-
	15	12.5 ± 4.5 C'	2.48 ± 1.27 D'	14.1 ± 1.9 A'
	20	98.3 ± 1.1 A'	26.11 ± 2.36 C'	12.2 ± 0.9 A'B'
	25	93.3 ± 3.7 A'	41.67 ± 4.65 B'	7.7 ± 0.7 C'
	30	100.0 ± 0.0 A'	60.95 ± 1.45 A'	5.9 ± 0.2 C'
	35	47.5 ± 13.2 B'	19.35 ± 5.91 C'	11.7 ± 1.1 B'

^w Values are the mean of two experiments, with five leaf-replicates per temperature-inoculum density combination and experiment. For each ID means followed by the same letter did not differ significantly ($P = 0.05$) according to the Tukey's HSD mean comparison test.

^x Disease severity at the end of incubation period (21 days after inoculation).

^y SAUDPC: Standardized area under the disease progress curve (AUDPC divided by the length of incubation; 21 days).

^z -: disease symptoms were not observed.

Table 3 Description and parameters of models fitted to the bacterial spot disease progress curves

Model ^y	Linearized equation ^z	b_0	r	R^2	MSE	R^{2*}
Monomolecular	$\ln\left(\frac{1}{1-y}\right) = b_0 + r_M CDD$	-1.4633	0.0083	0.670	0.343	0.688
Exponential	$\ln(y) = b_0 + r_E CDD$	-3.2572	0.0074	0.545	0.462	0.538
Logistic	$\ln\left(\frac{y}{1-y}\right) = b_0 + r_L CDD$	-4.7206	0.0157	0.699	1.075	0.784
Gompertz	$-\ln[-\ln(y)] = b_0 + r_G CDD$	-2.7869	0.0112	0.715	0.511	0.778

^y Models were fitted to pooled disease severity data from *Prunus* leaves inoculated with 10^8 CFU/ml suspensions of *X. arboricola* pv. *pruni* CFBP 5563 and incubated for 21 days at 20, 25 and 30°C for disease development. Data from two independent experiments were used.

^z Adapted from Campbell and Madden (1990). y : disease severity (0-1); b_0 and r : intercept and slope parameters of the linearized forms of the models; CDD : cumulative degree day; R^2 and MSE : coefficient of determination and mean square error of linear regression; R^{2*} : coefficient of determination between predicted back-transformed values and observed values.

Figure 1

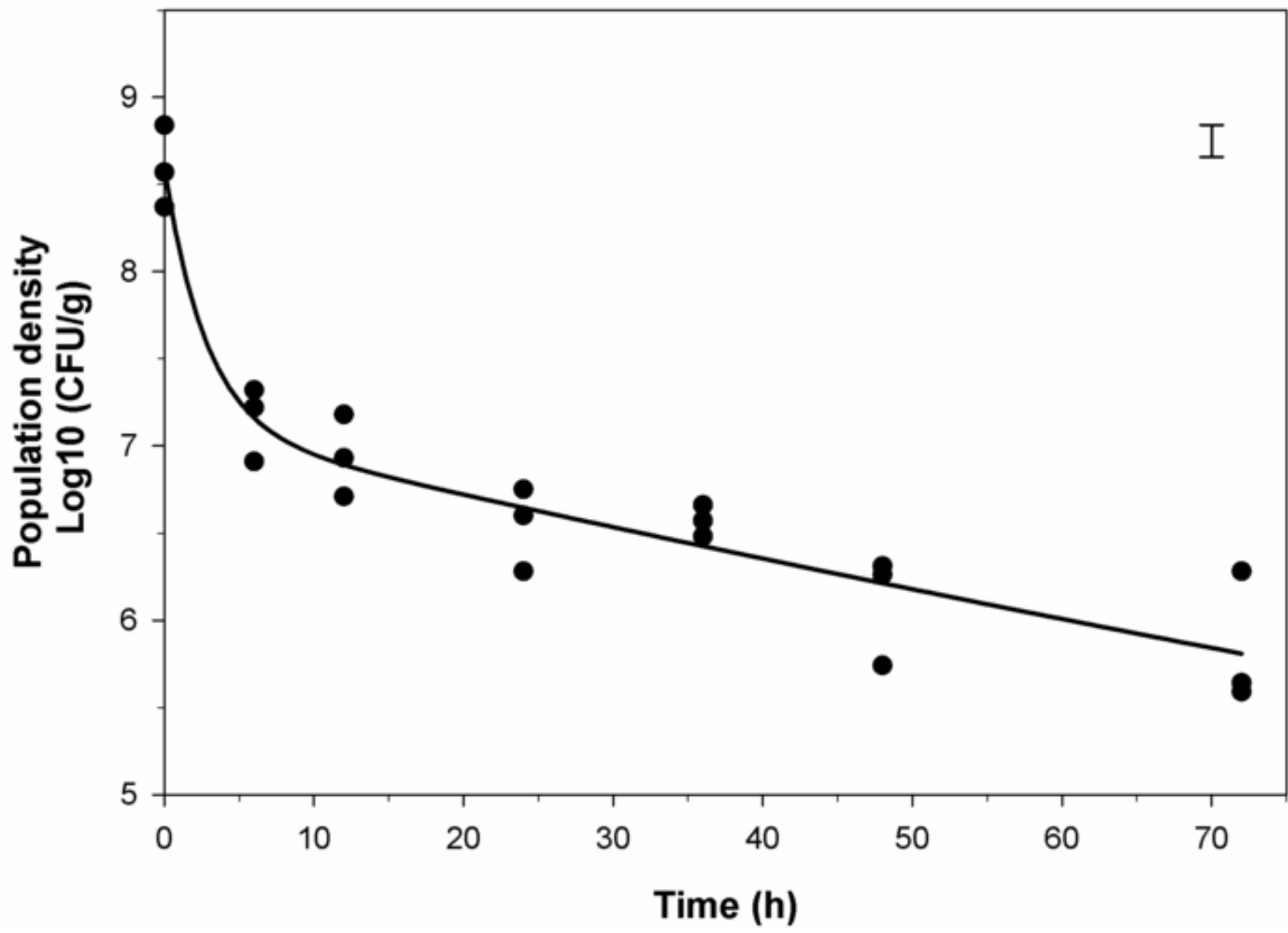


Figure 2

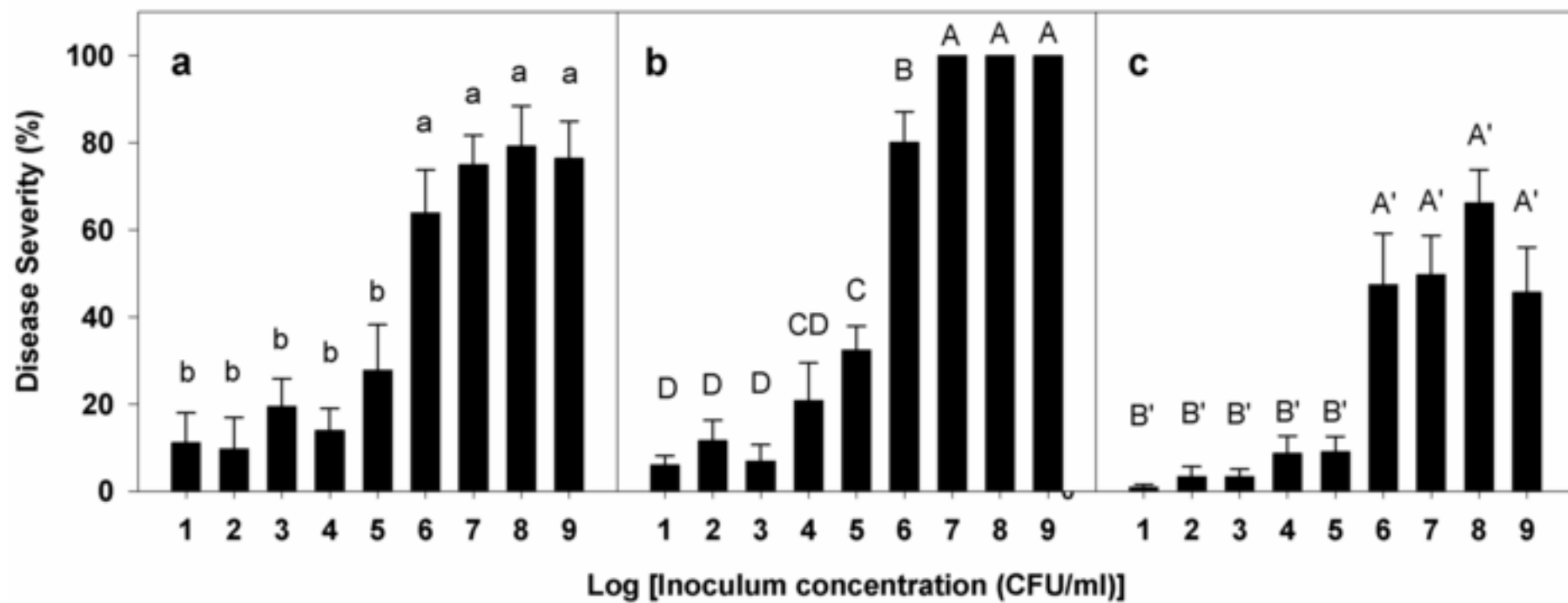


Figure 3

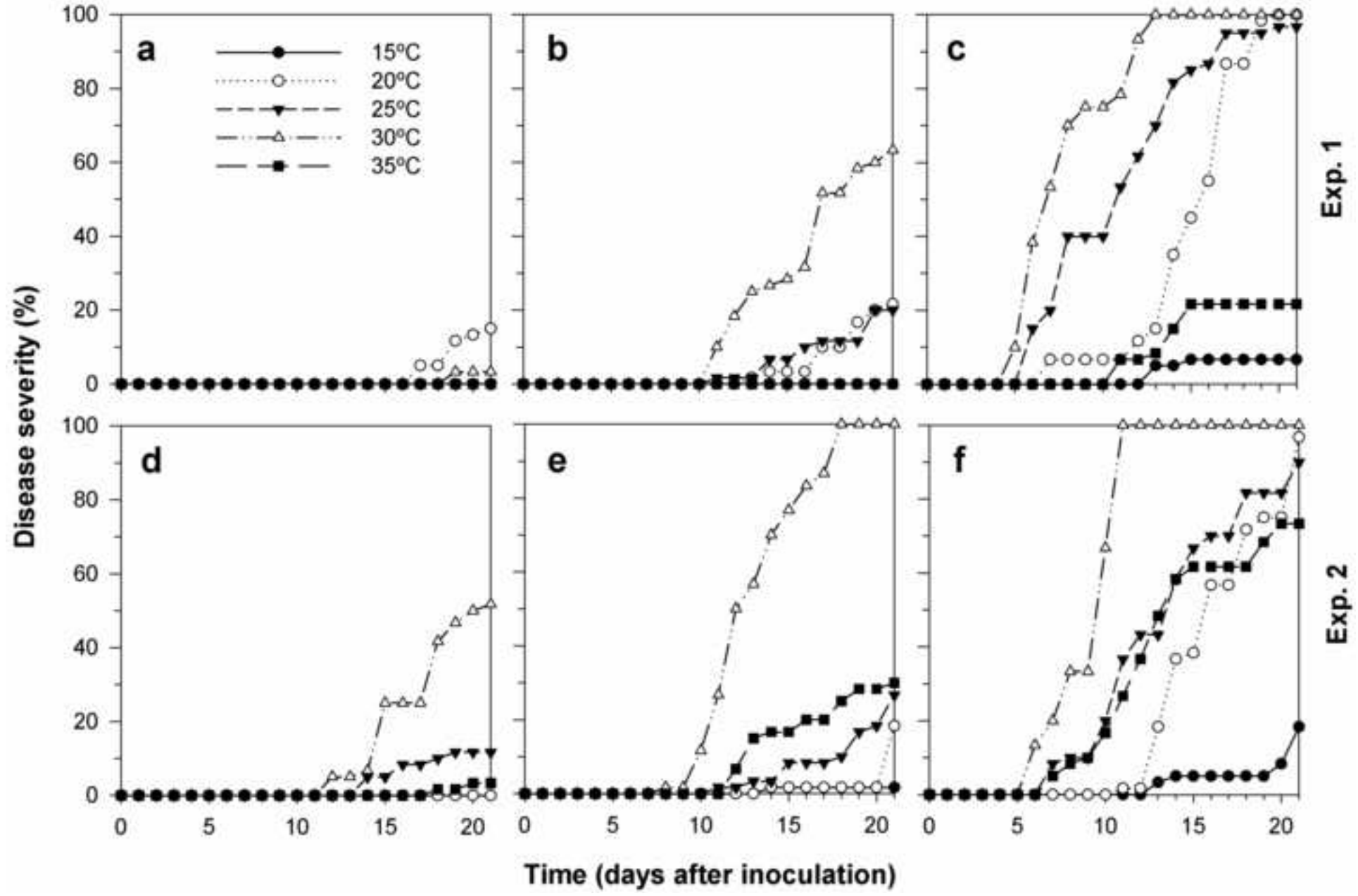


Figure 4

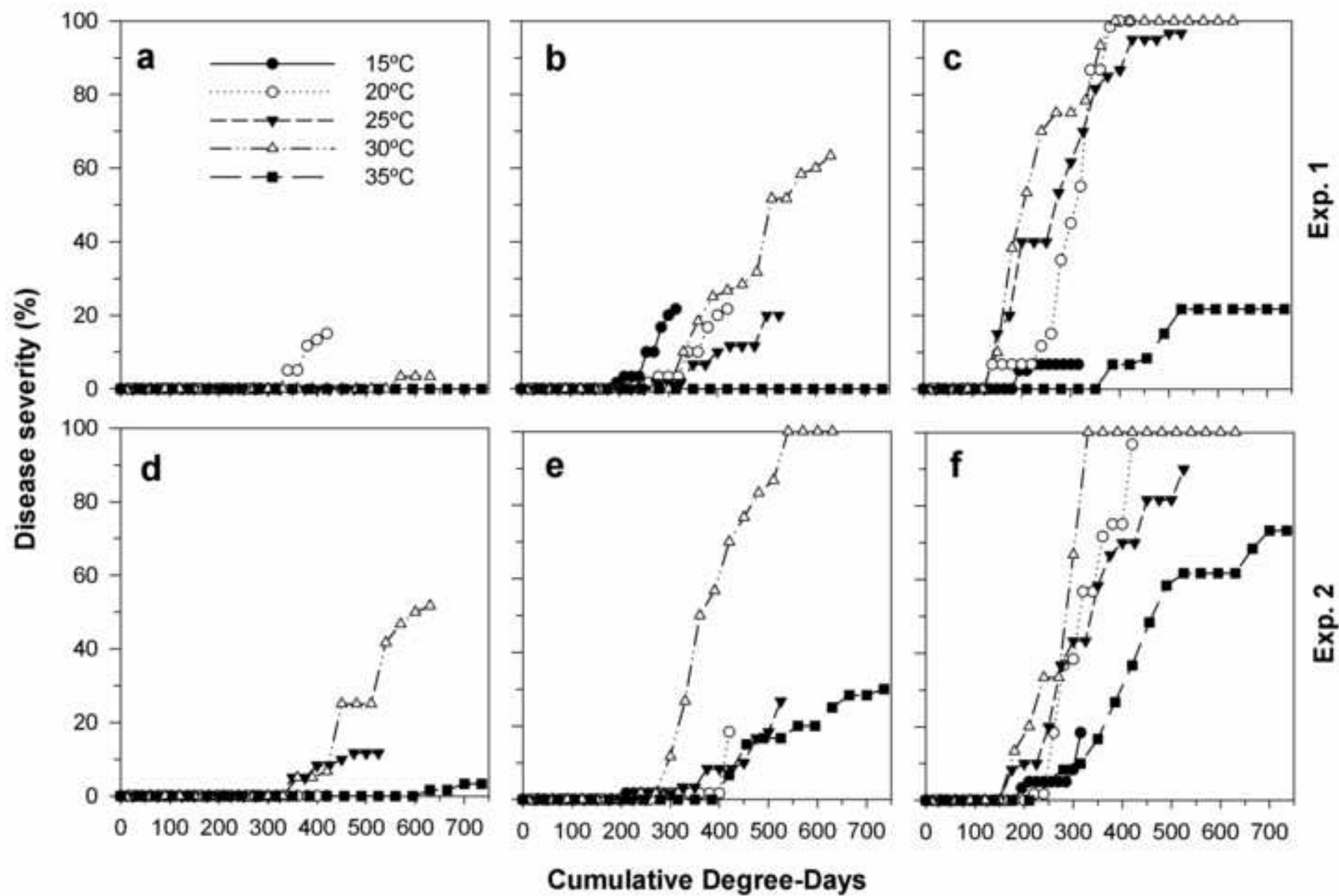


Figure 5

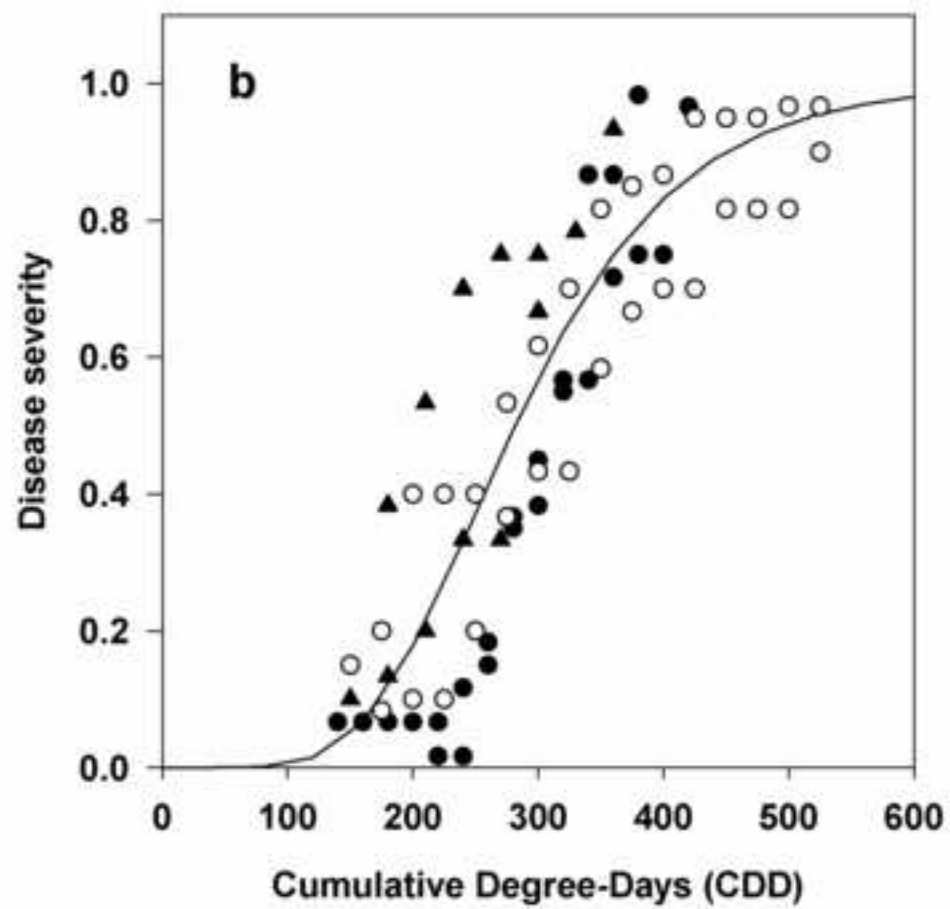
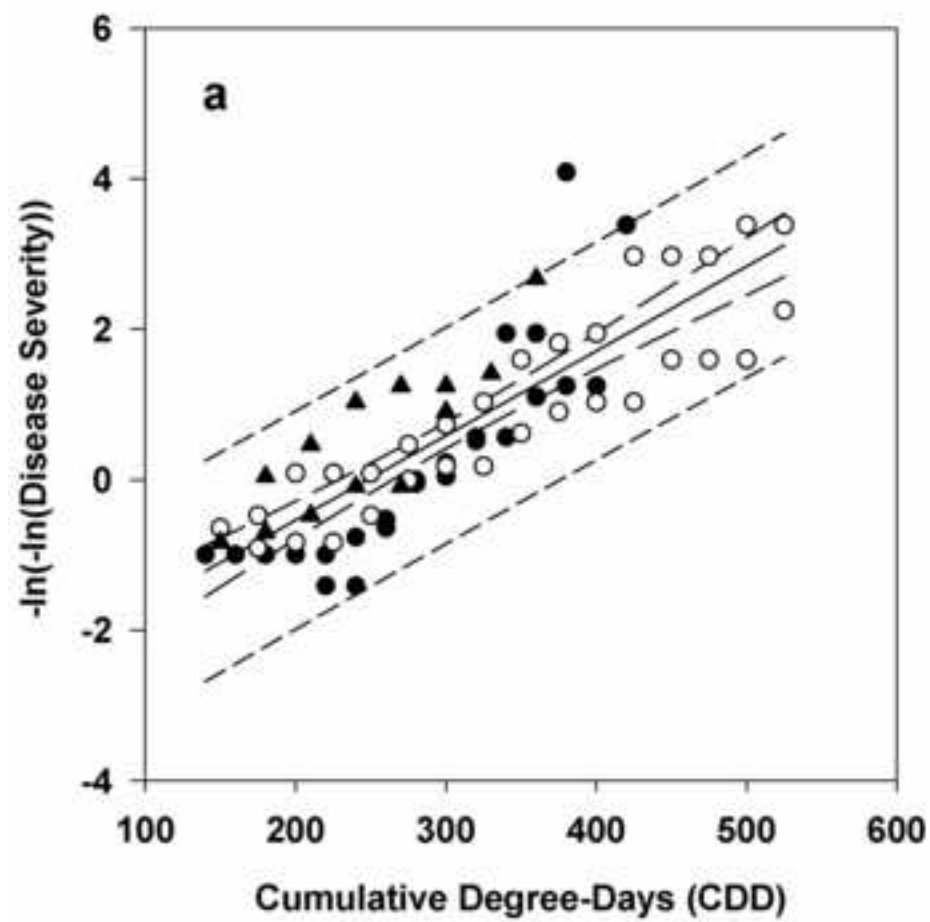


Figure 6

